

Angular profile of emission of non-zero spin fields from a higher-dimensional black hole

M. Casals^{1,2}, S. R. Dolan³, P. Kanti⁴ and E. Winstanley⁵

¹ *School of Mathematical Sciences, Dublin City University, Glasnevin, Dublin 9, Ireland*

² *CENTRA, Instituto Superior Técnico, Lisbon, Portugal*

³ *School of Mathematical Sciences, University College Dublin, Belfield, Dublin 4, Ireland*

⁴ *Division of Theoretical Physics, Department of Physics, University of Ioannina, Ioannina GR-451 10, Greece*

⁵ *School of Mathematics and Statistics, The University of Sheffield, Hicks Building, Hounsfield Road, Sheffield S3 7RH, United Kingdom*

Abstract

Recent works have included the effect of rotation on simulations of black hole events at the LHC, showing that the angular momentum of the black hole cannot be ignored and it makes a non-trivial contribution for most of the lifetime of the black hole. A key consequence of the rotation of the black hole is that the Hawking radiation is no longer isotropic, making it more difficult to infer space-time parameters from measurements of the emitted particles. In this letter we study the angular distribution of the Hawking emission of non-zero spin particles with specific helicity on the brane. We argue that the *shape* of the distribution could be used as a measure of the angular momentum of the black hole.

1 Introduction

Over the past ten years, there has been a huge amount of research into theories with Large Extra Dimensions [1], where the Standard Model matter fields are confined to a four-dimensional hyper-surface (or *brane*), with only gravitational degrees of freedom permitted to propagate in the higher-dimensional bulk.

One consequence of these theories is that the fundamental energy scale of quantum gravity, M_* , is related to the four-dimensional Planck energy M_P by $M_*^{2+n} \sim M_P^2 R^{-n}$, where R and n are the size and number of extra dimensions respectively. This means that M_* may be as small as $\mathcal{O}(\text{TeV})$, raising the exciting prospect of observing quantum gravity effects in the near future (see the reviews [2, 3, 4] for details and references).

Amongst quantum gravity processes, the potential to create higher-dimensional black holes in trans-Planckian particle collisions at the LHC has attracted intense interest in the literature. It is anticipated that such mini black holes will evaporate very quickly, due to

Hawking radiation [5]. Theoretically, the evaporation of higher-dimensional mini black holes is modelled in terms of four stages: the so-called ‘balding’, ‘spin-down’, ‘Schwarzschild’, and ‘Planck’ phases [2]. Of these, the ‘Schwarzschild’ phase is the simplest to study and the Hawking emission during this phase has been analyzed in depth by a number of authors, using both analytical [6, 7] and numerical [8, 9] techniques.

The ‘spin-down’ phase of the evolution has received considerable attention recently [10, 11, 12, 13, 14, 15]. A complete analysis of the ‘spin-down’ phase is lacking because the graviton emission has yet to be fully modelled (see [16] for work in this direction), leaving open the question of whether the idea that “black holes radiate mainly on the brane” [17] is valid for this phase of the evolution (see [8, 12, 18] for some papers discussing this issue).

The effect of including the ‘spin-down’ phase in simulations of black hole events at the LHC has recently been examined in detail [19] (for an earlier work, see [20]). It is found that, even if the black hole loses a substantial amount of angular momentum during the ‘balding’ phase, the ‘spin-down’ phase makes a significant difference to the properties of black hole events, which cannot be adequately approximated by the isotropic evaporation of the ‘Schwarzschild’ phase. Another key finding of [19] is that the ‘spin-down’ phase is not, as previously thought, short-lived compared with the ‘Schwarzschild’ phase (in fact, it is not possible to fully distinguish a separate ‘Schwarzschild’ phase, with the rotation of the black hole being significant for most of its lifetime).

The significance of the ‘spin-down’ phase complicates black hole events at the LHC [19], making their detection more challenging. It also means that measuring all the parameters describing a particular black hole event is likely to be very difficult. Our purpose in this letter is to investigate a key difference in the evaporation during the ‘spin-down’ phase compared with the ‘Schwarzschild’ phase, namely the non-isotropy of the emission. We are seeking aspects of the anisotropic emission which are particularly sensitive to the parameters describing the higher-dimensional black hole, with the intention that this will aid the development of detection and measurement strategies using full Monte-Carlo simulations [19].

The structure of this paper is as follows. In section 2, we briefly review the mathematical description of the higher-dimensional rotating black hole and Hawking radiation from it. In section 3 we consider the emission, on the brane, of positive and negative helicity spin-1/2 and spin-1 particles. We focus on the angular distribution of the emitted energy by these particles, and how this depends on the energies of the individual emitted particles, the angular momentum of the black hole, and the number of extra dimensions. Finally, in section 4, we present our conclusions, making some remarks on the prospects of using our results to determine some of the properties of rotating higher-dimensional black holes at the LHC.

2 Theoretical background and field equations

The gravitational field around a $(4 + n)$ -dimensional uncharged rotating black hole is described by the well-known Myers-Perry solution [21]. The projected line-element follows by fixing the values of the additional angular coordinates describing the extra space-like dimensions [2].

Then, the gravitational field on the brane takes the form

$$ds^2 = - \left(1 - \frac{\mu}{\Sigma r^{n-1}}\right) dt^2 - \frac{2a\mu \sin^2 \theta}{\Sigma r^{n-1}} dt d\varphi + \left(r^2 + a^2 + \frac{a^2 \mu \sin^2 \theta}{\Sigma r^{n-1}}\right) \sin^2 \theta d\varphi^2 + \frac{\Sigma}{\Delta} dr^2 + \Sigma d\theta^2, \quad (1)$$

where

$$\Delta = r^2 + a^2 - \frac{\mu}{r^{n-1}}, \quad \Sigma = r^2 + a^2 \cos^2 \theta. \quad (2)$$

We have also assumed that the black hole metric has only one non-zero angular momentum component, in a plane parallel to the brane, as we are interested in black holes created by the collision of particles on the brane. The mass M_{BH} of the black hole and its angular momentum J are then proportional to μ and $a\mu$, respectively,

$$M_{BH} = \frac{(n+2)A_{n+2}}{16\pi G} \mu, \quad J = \frac{2}{n+2} M_{BH} a, \quad (3)$$

where $A_{n+2} = 2\pi^{(n+3)/2}/\Gamma[(n+3)/2]$ is the area of an $(n+2)$ -dimensional unit sphere, and G is the $(4+n)$ -dimensional Newton's constant. By demanding that the impact parameter between the colliding particles is small enough for a black hole to be created, an upper bound can be imposed on the angular momentum parameter a as follows: we have $a_* \leq a_*^{max} = n/2 + 1$ [4], where $a_* = a/r_h$. The radius of the black hole's event horizon r_h is the largest, positive root of $\Delta(r) = 0$, and, for $n \geq 1$, there is only one such root in the region $r > 0$, which may be implicitly written as $r_h^{n+1} = \mu/(1 + a_*^2)$.

The four-dimensional background (1) is the one felt by the brane-localized Standard Model fields and thus the one that should be used for the derivation of the field equations for scalars, fermions and gauge bosons. By using the Newman-Penrose formalism and generalizing Teukolsky's four-dimensional analysis [22], one may derive a 'master' partial differential equation for the field perturbation Ψ_h on the brane [2, 10, 11]. Here, h is the helicity, or spin-weight, $h = (-|s|, +|s|)$, that we use to distinguish the radiative components of the spin- s field. The brane 'master' equation for the particular background (1) turns out to be separable - by using a factorized ansatz for the field perturbation expressed as a Fourier mode series

$$\Psi_h(t, r, \theta, \varphi) = \sum_{\Lambda} {}_h a_{\Lambda} {}_h R_{\Lambda}(r) {}_h S_{\Lambda}(\theta) e^{-i\omega t} e^{im\varphi}, \quad (4)$$

where ${}_h a_{\Lambda}$ are the Fourier coefficients, we write $\Lambda = \{lm\omega\}$ to denote the set of 'quantum numbers' of each mode, and ${}_h S_{\Lambda}$ are the spin-weighted spheroidal harmonics, the 'master' equation leads to two decoupled ordinary differential equations, namely

$$0 = \Delta^{-h} \frac{d}{dr} \left(\Delta^{h+1} \frac{d {}_h R_{\Lambda}}{dr} \right) + \left[\frac{K^2 - ihK\Delta'(r)}{\Delta} + 4ih\omega r + h(\Delta''(r) - 2)\delta_{h,|h|} - {}_h \lambda_{\Lambda} \right] {}_h R_{\Lambda}, \quad (5)$$

and

$$0 = \left[\frac{d}{dx} \left((1-x^2) \frac{d} {dx} \right) + a^2 \omega^2 (x^2 - 1) + 2ma\omega - 2hma\omega x - \frac{(m+hx)^2}{1-x^2} + {}_h \lambda_{\Lambda} + h \right] {}_h S_{\Lambda}(x). \quad (6)$$

In the above, we have defined the quantities $K = (r^2 + a^2)\omega - am$ and $x = \cos \theta$, and ${}_h \lambda_{\Lambda}$ is the constant of separation between the radial and angular equations.

The black-hole background (1) emits elementary particles on the brane in the form of Hawking radiation with temperature

$$T_H = \frac{(n+1) + (n-1)a_*^2}{4\pi(1+a_*^2)r_h}. \quad (7)$$

In this letter, we focus on the power emission rate, that may be expressed in two forms: in terms of unit time and energy and integrated over all angles θ

$$\frac{d^2 E}{dt d\omega} = \frac{1 + \delta_{|s|,1}}{2\pi} \sum_{l=|s|}^{\infty} \sum_{m=-l}^{+l} \frac{\omega}{\exp(\tilde{\omega}/T_H) \pm 1} \mathbf{T}_\Lambda, \quad (8)$$

or in terms of unit time, frequency and angle of emission,

$$\frac{d^3 E}{d(\cos\theta) dt d\omega} = \frac{1 + \delta_{|s|,1}}{4\pi} \sum_{l,m} \frac{\omega}{\exp(\tilde{\omega}/T_H) \pm 1} \mathbf{T}_\Lambda (-_h S_\Lambda^2 + {}_h S_\Lambda^2). \quad (9)$$

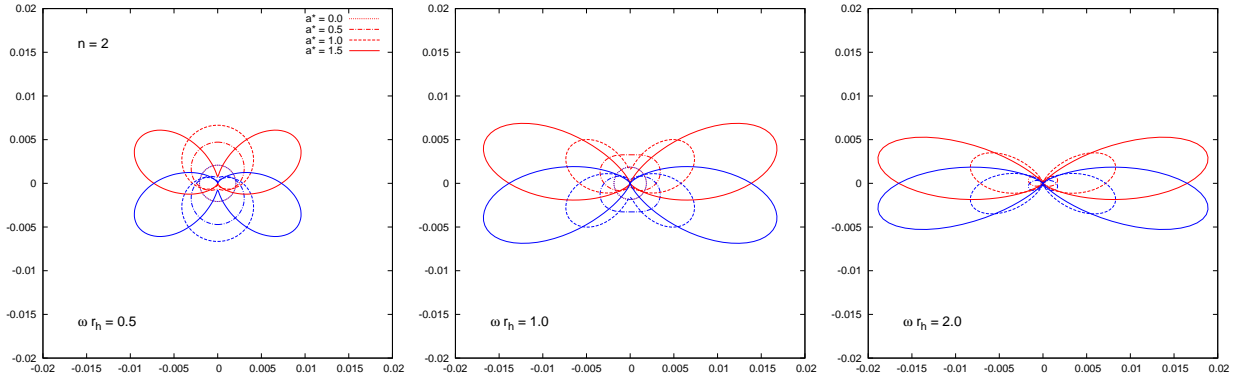
In the above expressions, $\tilde{\omega} = \omega - am/(a^2 + r_h^2)$ and ± 1 is a statistics factor for fermions and bosons, respectively. The extra factor $\delta_{|s|,1}$ in the emission rates for gauge bosons comes from the two linearly independent polarization states of the spin-1 field. Finally, the quantity \mathbf{T}_Λ is the transmission probability, defined as the flux of energy transmitted down the event horizon over the incident flux of energy on the black hole – it is this quantity that modifies the form of the radiation spectra of a black hole from the purely thermal one of a black body. For details of the derivation and computation of the emission rates (8, 9), including the numerical techniques used in solving the differential equations (5, 6), we refer the reader to Refs. [10, 11].

In Refs. [10, 11], the emission rates for scalars, fermions and gauge bosons were studied in detail. Amongst the results in those papers, it was found that the emitted power was significantly enhanced with both n and a_* - the enhancement factor for all species of particles was of order $\mathcal{O}(100)$ as n changed from 1 to 6, and of order $\mathcal{O}(10)$ as a_* increased from zero towards its maximum value a_*^{max} . The differential emission rate per unit time, frequency and angle of emission (9) was also studied. The angular variation in the spectra was characterized by two main features: in the low-energy regime, the spin-rotation coupling for fermions and gauge bosons caused the polarization of the emitted radiation in directions nearly parallel to the rotation axis; as either the angular momentum of the black hole and/or the energy of the emitted particle increased, this feature receded and the centrifugal force caused the concentration of the emitted radiation, for all species of particles, on the equatorial plane, i.e. transversely to the rotation axis of the black hole.

3 The angular profile

In this section, we will investigate further the angular profile of the emitted radiation on our brane from a higher-dimensional black hole by focusing on the emission of individual helicity modes. We will therefore consider only the emission of brane-localized fermions and gauge bosons, and ignore henceforth the single-component scalar fields. In each case, the energy flux for positive helicity particles is obtained from (9) by including only the term with $_{-|s|}S_\Lambda^2$; similarly the energy flux for negative helicity particles is obtained from the $_{+|s|}S_\Lambda^2$ term in (9) [23].

Fermions



Vector Bosons

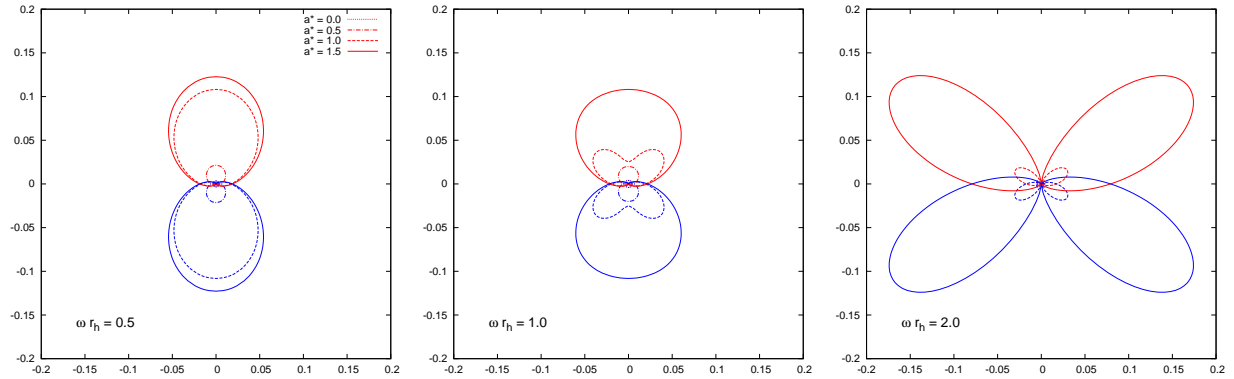


Figure 1: Polar plots depicting the emitted differential power rate (9) of individual helicities for brane localized fermions (top) and vector bosons (bottom) in terms of the angle. The red curves denote positive helicity emission and the blue curves negative helicity. The number of extra dimensions is fixed by $n = 2$, and we have plotted the angular distribution for different ωr_h , and for four values of the angular momentum parameter a_* . In each case the distance of a point on a curve from the origin is the magnitude of the power emitted in that direction.

The study of the differential emission rate (9) for spin-1/2 and spin-1 particles of Ref. [11] considered only the ‘total’ emission, i.e. the sum of the emission of both helicity modes in each case. The spin-weighted spheroidal harmonics satisfy the property (after an overall choice of sign)

$${}_h S_\Lambda(\theta) = (-1)^{l+m} {}_{-h} S_\Lambda(\pi - \theta). \quad (10)$$

As a result, the sum of the squared values of the spin-weighted spheroidal harmonics for the two helicities $h = (-|s|, |s|)$ is bound to be symmetric under the change $\pi \rightarrow \pi - \theta$, and the plots showing the angular variation in the ‘total’ emission are symmetric in the two hemispheres. However, it is clear that the emission of single-helicity modes is not going to have the same property, and it is this additional variation in the angular distribution that we investigate here. With a similar motivation, certain aspects of the angular distribution of the emission spectra of spin-1/2 particles were studied also in [15].

In Fig. 1, we present a set of polar plots for the differential power emission rate (9) for fermions (top) and gauge bosons (bottom) in terms of the emitted latitudinal angle θ . The two colour schemes represent the two opposite helicities $h > 0$ (red) and $h < 0$ (blue). The three plots for each type of particle correspond to different values of the energy channel ($\omega r_h =$

0.5, 1.0, 2.0), four values of the angular-momentum parameter of the black hole ($a_* = 0.0, 0.5, 1.0$ and 1.5) and fixed number of additional space-like dimensions ($n = 2$). The rotation axis in these plots runs vertically. For each curve in the graphs in Fig. 1, the distance of a point on a curve from the origin is the magnitude of the power emitted in that direction. For each value of the emitted particle energy, the emission in the zero-angular-momentum case $a_* = 0$ is isotropic as expected, and represented by a small circle in the centre of the plots.

From Fig. 1, we observe that for low values of the energy of the emitted particle and small black hole angular momentum a_* , the two helicity modes are indeed aligned to the rotation axis of the black hole, in accordance to the behaviour found in [11], but with the two helicity ‘jets’ facing towards opposite sides. Positive helicity particles are emitted in the ‘northern’ hemisphere (i.e. pointing in the same direction as the angular velocity vector of the black hole), while negative helicity particles are emitted in the ‘southern’ hemisphere. We also note the order of magnitude increase in the emitted power in spin-1 particles compared with spin-1/2 particles.

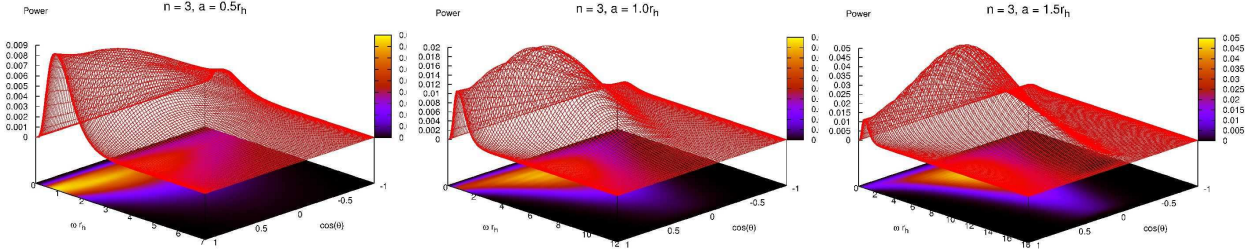
As the energy of the emitted particles is increased, or if the black hole angular momentum a_* is very large, this pattern is destroyed: although the preference shown by each helicity mode towards one of the hemispheres is still prominent, the emission is now concentrated in two directions at almost 45 degrees to the rotation axis. This effect is stronger for fermions than for the gauge bosons. The energy at which this effect becomes apparent increases as the angular momentum of the black hole decreases: for large $a_* = 1.5$, the ‘jets’ at 45 degrees have formed even when ωr_h is as low as 0.5, while for small $a_* = 0.5$, we see these ‘jets’ at 45 degrees only when ωr_h is nearer 2. As the energy increases further, the asymmetry in the emission between the two helicity modes becomes gradually less prominent with the emission concentrating more and more on the equatorial plane.

It can also be seen from Fig. 1 that increasing a_* increases the magnitude of the power emitted, particularly for higher energy modes (and hence increases the number of particles emitted, as observed in [15]). There is also a certain degeneracy in the shape of the curves, for example, the curves for fermion emission with $(a_* = 1.5, \omega r_h = 0.5)$ and $(a_* = 1.0, \omega r_h = 1)$ are very similar. However, since the energy of the emitted particles can be measured experimentally, this degeneracy can be broken.

To explore the dependence of the angular distribution on the particle energy further, in Fig. 2, we have plotted the emitted power for positive helicity fermions (top) and gauge bosons (bottom) as a function of the frequency ωr_h and $\cos\theta$, considering three different values for the angular-momentum parameter ($a_* = 0.5, 1.0, 1.5$) and fixed dimensionality of space-time ($n = 3$). For smaller non-zero values of a_* , almost all of the radiation of the individual helicity mode is emitted in directions nearly parallel to the rotation axis of the black hole with a clear preference towards one of the hemispheres; the effect is more marked for spin-1 particles, as might be expected from the increased spin-orbit coupling due to the increased internal spin of the vector bosons compared with the fermions. As a_* increases, the power emission curve for fermions becomes higher, as expected, and also more and more radiation is concentrated on the equatorial plane rather than in directions nearly parallel to the rotation axis. However, for spin-1 particles, we can see in Fig. 2 that, while for vector bosons emitted with higher energies there is evidence for the emission tending to be nearer the equatorial plane than the axis, the majority of the emission in lower-energy particles is still very much concentrated in directions nearly parallel to the axis of rotation.

Therefore, the emission of lower-energy bosons in directions nearly parallel to the axis of

Fermions



Vector Bosons

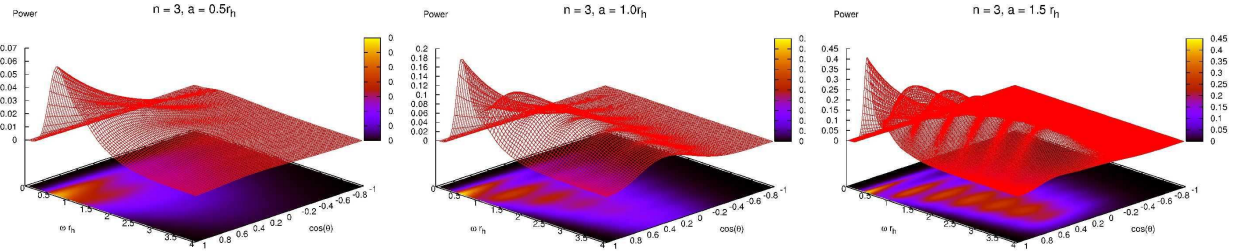


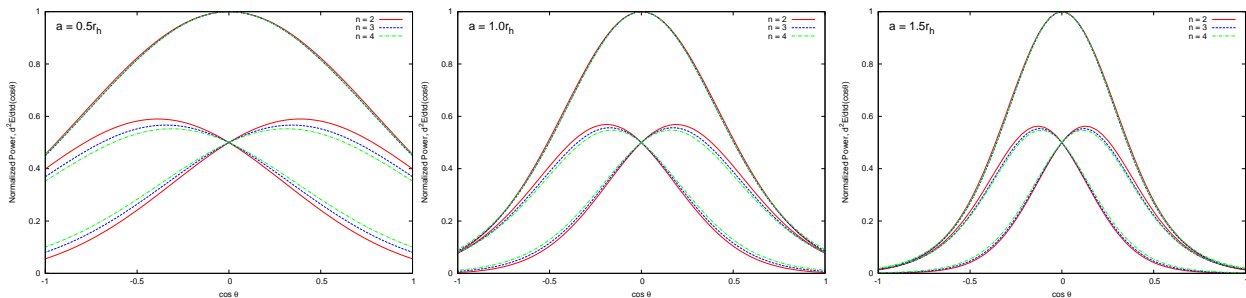
Figure 2: Power-versus-frequency-versus-angle plots for positive helicity fermion (top) and vector boson (bottom) emission, for $n = 3$, and $a_* = 0.5, 1.0, 1.5$.

rotation may provide the best means of measuring the direction of the axis of rotation. On the other hand, if the energy of the emitted fermions is accurately measured, the proportion of the emitted radiation in directions nearly parallel to the rotation axis and close to the equatorial plane (whose directions can, at least in theory, be determined from the vector boson emission) can give us an estimate for the angular-momentum of the black hole (see also [15] for a discussion of this measurement).

Thus far we have not considered the role the number of extra dimensions plays in this angular distribution. In the case of the ‘total’ emission rates, where the contribution from both helicity modes was considered, the dependence on a_* and n was also very prominent, however, as both parameters caused the same effect in the spectra, namely their enhancement, it was impossible to distinguish their role. In Fig. 3, we present a set of plots of the energy emissivity of the black hole integrated over the frequency ωr_h , in terms of the emitted angle for three different values of the angular momentum parameter ($a_* = 0.5, 1.0, 1.5$), and for three different values of the number of extra dimensions ($n = 2, 3, 4$) in each case. The purpose is to investigate the dependence of the *shape* of the curves on n , rather than the magnitude of the emission. To this end, we rescale our data so that the peak of the emission curve for the sum of the two helicity modes is at unity at $\theta = \pi/2$ with the rescaled integrated emissivity curves for each helicity mode shown below.

The spin-1 profiles in Fig. 3 vary more than the spin-1/2 profiles as the number of extra dimensions, n , changes, but none of the profiles change a great deal except in the spin-1 case when the angular momentum of the black hole is comparatively small ($a_* = 0.5$). From this we conclude that the angular distribution of emitted particles is not a good indicator of the number of extra dimensions. However, this also means that the angle-dependent spectra carry a strong dependence only on the angular momentum parameter, and this opens the way for the

Fermions



Vector Bosons

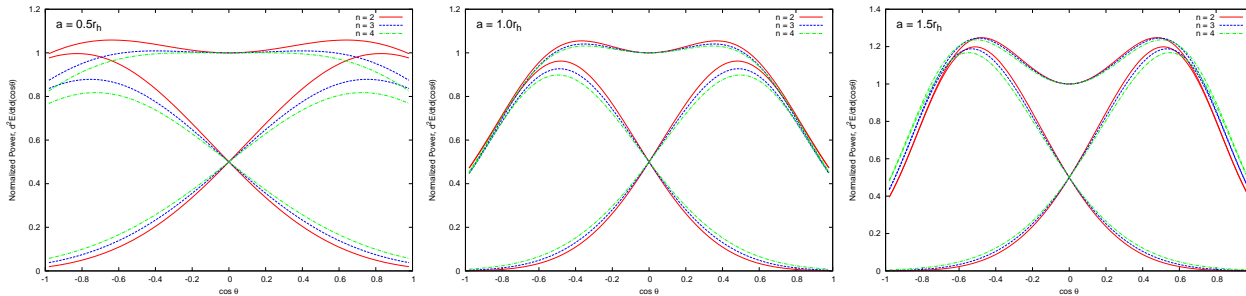


Figure 3: Energy emissivity integrated over frequency ωr_h , for fermions (top) and vector bosons (bottom) as a function of angle, for $n = 2, 3, 4$, and $a_* = 0.5, 1.0, 1.5$. The power has been normalized so that the total emission when $\theta = \pi/2$ is equal to unity. In each plot, the upper curve corresponds to the emission rate of the sum of both helicities and the two lower ones to the ones of the two individual helicities.

determination of a_* . From Fig. 3, we see that the profiles of the individual helicity particles are more sharply peaked for spin-1 compared with spin-1/2 particles, at the same value of a_* , but, interestingly, the total power emission (summing over the two helicities) has a broader shape in the spin-1 case compared with the spin-1/2 case, for all values of a_* .

The authors of [15] also studied the angular distribution of the flux of negative helicity fermions, but for a particular value of the frequency ωr_h . Fig. 2 confirms, for all frequencies in the power flux, their observation for the fermion particle flux that there is an asymmetry in the emission in helicity-dependent states, which becomes more strongly peaked as the angular-momentum parameter a_* increases. From Fig. 3, it can also be seen that the asymmetry in the power flux decreases as the number of extra dimensions n increases, which was found to be the case for the fermion particle flux at a particular frequency in [15].

4 Discussion and conclusions

The possibility of creating higher-dimensional black holes at the LHC and subsequently observing their Hawking radiation is one of the most exciting consequences of models with Large Extra Dimensions. The recent inclusion of black hole angular momentum in simulations of such black hole events [19, 20], as well as improving the accuracy of the simulations, has also indicated that black hole rotation is likely to have major consequences for the detection of Hawking radiation. This is particularly true for the emission, on the brane, of particles with

non-zero spin, which, in practice, are the main particles which will be detected should black holes be formed at the LHC.

The primary consequence of including black hole rotation is that the Hawking emission is no longer isotropic [11, 13, 15]. In this letter we have examined further the nature of this anisotropy for particles of spin-1/2 and spin-1, considering separately the positive and negative helicity states, to determine whether any features of the anisotropic emission could, at least in principle, be used to derive information about the evaporating black hole or the higher-dimensional space-time.

There are three main space-time parameters which it would be desirable to probe in black hole events: the number of extra dimensions n , the size of the extra dimensions R , and the energy scale of quantum gravity M_* . These will be the same for all black hole events, so a large number of events can be used in their determination. In addition, one would be interested, for individual black hole events, in measuring the mass M and angular momentum J of the black hole when it is first formed (or, equivalently, r_h and a_*).

The question of how to extract information about these parameters from the Hawking radiation is still not completely resolved. For rotating black holes, since increasing either n or a_* increases the Hawking flux, disentangling this degeneracy in the values of n and a_* from, for example, the numbers of emitted particles, may be difficult. In this paper, we have found that, for both fermion and gauge boson emission, the shape of the angular distribution of total energy emission for both positive and negative helicity particles depends only weakly on the number of extra dimensions n , for all values of the black hole angular momentum parameter a_* . This means that the shape cannot be used to measure the value of n , with only the magnitude of the power emitted depending strongly on its value. On the other hand, the angular distribution of energy emission for both species of particles was found to depend strongly on a_* and can therefore be used as a good indicator of the angular momentum of the produced black hole. By measuring a_* for many black hole events, it would be possible to build up a distribution of $a_* < a_*^{max}$.

Another interesting measurement would be the direction of the axis of rotation of the black hole. Rotating black holes preferentially emit spin-1 particles over fermions (with approximately an order-of-magnitude greater energy emission) and low-energy spin-1 particles are emitted almost entirely in directions nearly parallel to the axis of rotation, particularly for smaller values of n . On the other hand, the fermion energy emission is strongly peaked on the equatorial plane, providing complementary evidence for the direction of the axis of rotation [15]. Measuring particles of a specific helicity further refines this measurement by effectively indicating the ‘arrow’ of the black hole angular velocity vector along this axis.

In our study of the physics of Hawking emission from higher-dimensional black holes, we have taken the usual semi-classical approach of calculating the emission from a fixed black hole geometry. This does not model the evolution of the black hole during the evaporation process, with the black hole losing mass and angular momentum. It is also anticipated that the black hole will recoil as it emits particles [7], due to momentum conservation, and that the axis of rotation may well change direction. Every particle emitted, observed or unobserved, changes the mass and angular velocity of the black hole. In practice, the process is stochastic and hence each black hole decay is unique. Nevertheless, by combining the spectra of semi-classical theory with Monte Carlo methods (as in [19, 20]), one may model the likely ‘ensemble’ of black hole decays. This approach will be crucial for determining whether the physics effects we have described in this paper will be detectable in real data and for devising detection strategies.

Acknowledgements

We thank V. P. Frolov for useful discussions on this topic. MC and SRD gratefully acknowledge financial support from the Irish Research Council for Science, Engineering and Technology (IRCSET). The work of MC is partially funded by Fundação para a Ciência e Tecnologia (FCT) - Portugal, reference PTDC/FIS/64175/2006. PK acknowledges participation in RTN Universenet (MRTN-CT-2006035863-1 and MRTN-CT-2004-503369). EW thanks the School of Mathematical Sciences, University College Dublin, for hospitality while this work was completed. The work of EW is supported by STFC (UK), grant number ST/G000611/1.

References

- [1] N. Arkani-Hamed, S. Dimopoulos and G. R. Dvali, *Phys. Lett. B* **429**, 263 (1998) [hep-ph/9803315]; *Phys. Rev. D* **59**, 086004 (1999) [hep-ph/9807344];
I. Antoniadis, N. Arkani-Hamed, S. Dimopoulos and G. R. Dvali, *Phys. Lett. B* **436**, 257 (1998) [hep-ph/9804398].
- [2] P. Kanti, *Int. J. Mod. Phys. A* **19**, 4899 (2004) [hep-ph/0402168]; *Lect. Notes Phys.* **769**, 387 (2009) [arXiv:0802.2218 [hep-th]]; arXiv:0903.2147 [hep-th].
- [3] M. Cavaglia, *Int. J. Mod. Phys. A* **18**, 1843 (2003) [hep-ph/0210296];
G. L. Landsberg, *Eur. Phys. J. C* **33**, S927 (2004) [hep-ex/0310034];
K. Cheung, hep-ph/0409028;
S. Hossenfelder, hep-ph/0412265;
A. S. Majumdar and N. Mukherjee, *Int. J. Mod. Phys. D* **14**, 1095 (2005) [astro-ph/0503473].
- [4] C. M. Harris, hep-ph/0502005.
- [5] S. W. Hawking, *Commun. Math. Phys.* **43**, 199 (1975).
- [6] P. Kanti and J. March-Russell, *Phys. Rev. D* **66**, 024023 (2002) [hep-ph/0203223]; *Phys. Rev. D* **67**, 104019 (2003) [hep-ph/0212199].
- [7] V. P. Frolov and D. Stojkovic, *Phys. Rev. D* **66**, 084002 (2002) [hep-th/0206046].
- [8] C. M. Harris and P. Kanti, *JHEP* **0310**, 014 (2003) [hep-ph/0309054].
- [9] A. S. Cornell, W. Naylor and M. Sasaki, *JHEP* **0602**, 012 (2006) [hep-th/0510009];
V. Cardoso, M. Cavaglia and L. Gualtieri, *Phys. Rev. Lett.* **96**, 071301 (2006) [hep-th/0512002]; *JHEP* **0602**, 021 (2006) [hep-th/0512116];
S. Creek, O. Eftimiou, P. Kanti and K. Tamvakis, *Phys. Lett. B* **635**, 39 (2006) [hep-th/0601126];
D. C. Dai, N. Kaloper, G. D. Starkman and D. Stojkovic, *Phys. Rev. D* **75**, 024043 (2007) [hep-th/0611184].
- [10] G. Duffy, C. Harris, P. Kanti and E. Winstanley, *JHEP* **0509**, 049 (2005) [hep-th/0507274].

- [11] M. Casals, P. Kanti and E. Winstanley, *JHEP* **0602**, 051 (2006) [hep-th/0511163];
M. Casals, S. Dolan, P. Kanti and E. Winstanley, *JHEP* **0703**, 019 (2007) [hep-th/0608193].
- [12] S. Creek, O. Efthimiou, P. Kanti and K. Tamvakis, *Phys. Lett. B* **656**, 102 (2007) [arXiv:0709.0241 [hep-th]];
M. Casals, S. R. Dolan, P. Kanti and E. Winstanley, *JHEP* **0806**, 071 (2008) [arXiv:0801.4910 [hep-th]].
- [13] D. Ida, K. y. Oda and S. C. Park, *Phys. Rev. D* **67**, 064025 (2003) [Erratum-ibid. D **69**, 049901 (2004)] [hep-th/0212108]; *Phys. Rev. D* **71**, 124039 (2005) [hep-th/0503052]; *Phys. Rev. D* **73**, 124022 (2006) [hep-th/0602188].
- [14] V. P. Frolov and D. Stojkovic, *Phys. Rev. D* **67**, 084004 (2003) [gr-qc/0211055];
H. Nomura, S. Yoshida, M. Tanabe and K. i. Maeda, *Prog. Theor. Phys.* **114**, 707 (2005) [hep-th/0502179];
E. Winstanley, arXiv:0708.2656 [hep-th];
T. Kobayashi, M. Nozawa, Y. Takamizu, *Phys. Rev. D* **77**, 044022 (2008) [arXiv:0711.1395 [hep-th]];
S. Chen, B. Wang, R. K. Su and W. Y. Hwang, *JHEP* **0803**, 019 (2008) [arXiv:0711.3599 [hep-th]].
- [15] A. Flachi, M. Sasaki and T. Tanaka, arXiv:0809.1006 [hep-ph].
- [16] H. Kodama, *Prog. Theor. Phys. Suppl.* **172**, 11 (2008) [arXiv:0711.4184 [hep-th]]; *Lect. Notes Phys.* **769**, 427 (2009) [arXiv:0712.2703 [hep-th]];
J. Doukas, H. T. Cho, A. S. Cornell and W. Naylor, arXiv:0906.1515 [hep-th];
P. Kanti, H. Kodama, R. A. Konoplya, N. Pappas and A. Zhidenko, arXiv:0906.3845 [hep-th].
- [17] R. Emparan, G. T. Horowitz and R. C. Myers, *Phys. Rev. Lett.* **85**, 499 (2000) [hep-th/0003118].
- [18] E. Jung and D. K. Park, *Nucl. Phys. B* **731**, 171 (2005) [hep-th/0506204]; *Mod. Phys. Lett. A* **22**, 1635 (2007) [hep-th/0612043].
- [19] J. A. Frost, J. R. Gaunt, M. O. P. Sampaio, M. Casals, S. R. Dolan, M. A. Parker and B. R. Webber, arXiv:0904.0979 [hep-ph].
- [20] D-C. Dai, G. Starkman, D. Stojkovic, C. Issever, E. Rizvi, and J. Tseng, *Phys. Rev. D* **77**, 076007 (2008) [arXiv:0711.3012 [hep-ph]].
- [21] R. C. Myers and M. J. Perry, *Annals Phys.* **172**, 304 (1986).
- [22] S. A. Teukolsky, *Phys. Rev. Lett.* **29**, 1114 (1972); *Astrophys. J.* **185**, 635 (1973).
- [23] P. A. Bolashenko and V. P. Frolov, *Theor. Math. Phys.* **78**, 31 (1989);
M. Casals and A. C. Ottewill, *Phys. Rev. D* **71**, 124016 (2005) [arXiv:gr-qc/0501005].